Isothermal Oxidation Behaviours of FeAl Intermetallics In Ambient Air and Pure Oxygen

C-H. Xu and W. Gao*

Department of Chemical & Materials Engineering, The University of Auckland, New Zealand.

(Received January 17, 2000; final form March 27, 2000)

ABSTRACT

The oxidation behaviour of Fe-37Al intermetallics in ambient air and dry oxygen at 1273-1473K was investigated. Oxide products were studied by using X-ray diffraction, scanning electron microscopy, atomic force microscopy, and X-ray photoelectron spectroscopy. The results showed that the oxidation rates for the specimens oxidised in ambient air were higher than in oxygen. A two-layer oxide scale formed on the surface of Fe-37Al specimens during oxidation. For the oxidation in air, the outer layer was a convoluted α-Al_2O_3 layer with filamentary oxides and an inner layer consisting of Al_2O_3 + AlN. For the oxidation in oxygen, the outside was a convoluted α-Al_2O_3 layer and the inner layer was Al_2O_3. It is believed that the nitrogen ions in Al_2O_3 and the growth of filamentary oxides caused an increase of the oxidation rate in air.

Keywords: FeAl, intermetallics, high temperature oxidation, oxide, nitride

1. INTRODUCTION

Iron aluminium intermetallics, FeAl and Fe_3Al, possess good isothermal oxidation and sulphidation resistance /1/. They also offer advantages such as low material costs, conservation of strategic metals and lower densities than stainless steels or nickel alloys. However, their room temperature ductility is relatively poor and strength sharply drops above 873K. Recent researches indicated that the room temperature ductility and high temperature strength can be improved significantly /2,3/ and so these materials have attracted much attention in recent years.

We have recently studied the high temperature oxidation and sulphidation behaviours of Fe-Al, including isothermal and cyclic oxidation kinetics, scale structure and spallation tendency, and the reactive elements effects (REE), in an effort to use these materials in industrial applications /4,5,6/. The present paper reports the oxidation kinetics of Fe-37Al oxidised in ambient and dry oxygen atmospheres at temperature range of 1273-1473K, and the structures of the oxide layers formed on Fe-37Al intermetallics after oxidation.

2. EXPERIMENTAL PROCEDURE

The composition of the tested materials is 37at.%Al balanced with Fe. The cast ingots were annealed at 1373K for 86,400s for homogenisation. Specimens were cut from the ingots to the size of $10\times10\times1mm^3$, and polished with steps down to 3 μm diamond paste.

Thermogravimetric measurements (TGA) were used to study the oxidation kinetics. The oxidation experiments were performed in a SETRAM TG-DSC 92 thermal analyser at temperatures of 1273-1473K in ambient atmosphere and in dry oxygen flow for 180,000s (50 hours). The mass changes of the specimens were measured by an electronic balance with

* Corresponding author

an accuracy of 0.01mg. Then the oxidised specimens were cooled at rate of 0.3K/s to room temperature.

Oxide scales spalled away from the specimen surface during cooling stage. Characterisation of the spalled oxide scales and the specimen surfaces after spallation were conducted in a PHILLIPS 505 scanning electronic microscope (SEM). The surfaces of the specimens after oxide scale spallation were also examined by using an atomic force microscope (AFM). The spalled oxide scales and the specimens after oxide spallation were also examined with a PHILLIPS PW 1790 X-ray diffractometer (XRD) to obtain the information of crystal structures. Co Kα X-ray at 35kV and 40 mA was used.

The compositions and the chemical states of the elements on the surfaces of the specimens after oxide spallation were studied on a Kratos-XSAM X-ray photoelectron spectrometer (XPS). Mg Kα (hν = 1253.6 eV) was chosen as the excitation source. Spectrometer pass energies of 65 eV and 20 eV were chosen for detection of elements and for the identification of the chemical states of elements, respectively.

3. RESULTS

3.1 Isothermal Oxidation Kinetics

The oxidation kinetic curves for Fe-37Al oxidised at 1273-1473K in ambient and dry oxygen atmospheres are plotted in Figure 1, showing the mass gains versus exposure time for up to 180,000s. TGA experiments showed that all oxidation reactions of the Fe-37Al alloys at 1273-1473K obeyed an approximately parabolic rate law. The oxidation rates of Fe-37Al in ambient atmosphere were faster than in pure oxygen at all tested temperatures.

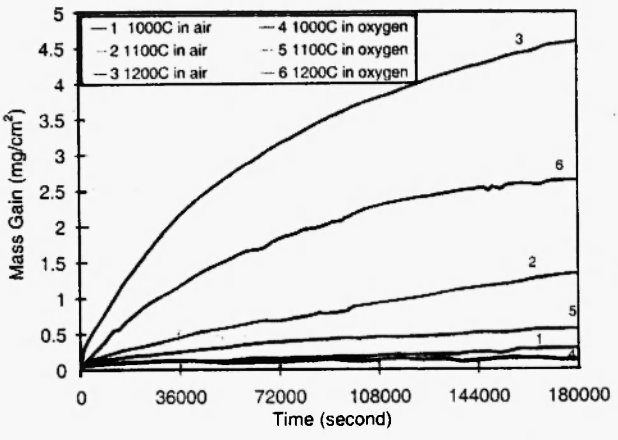

Fig. 1: Mass gains versus oxidation time for Fe-37Al specimens in ambient and dry oxygen atmospheres

3.2 Scale Microstructure

Figure 2 shows the morphologies of the oxide scales and the surface after scale spallation for Fe-37Al specimens oxidised in ambient air at 1373K for 180,000s. The morphology on the spalled scales showed convoluted feature with filamentary oxides, Figure 2(a). The surface of the specimens after oxide spallation showed a fine inner oxide layer formed on the substrate, Figure 2(b). The fine oxide layers on the surface of the oxidised specimens after scale spallation were imaged using AFM, Figure 2(c), showing an average grain size of ~100 nm.

Figure 3 shows the morphology of the oxide and the surface of the substrate after scale spallation for Fe-37Al specimens oxidised in oxygen. Convoluted oxide scales (Figure 3(a)) could be seen on the top surface of the spalled scales. But the scales do not have filamentary oxides on the top the specimens oxidised in oxygen. The morphology of the specimens after oxide spallation also showed a fine oxide layer on the substrate, Figure 3(b). The inner oxide layer was also imaged using AFM, Figure 3(c). The average size of the grains in this thin oxide layer was about 30 nm, Figure 3(d). The grain size of the inner oxide layer formed in oxygen was much smaller than that formed in air.

3.3 Compositional Analysis on Oxidised Specimens after Scale Spallation

The oxidation products were examined by X-ray diffraction, showing that the spalled oxide scales for oxidation in both ambient air and oxygen are α-Al_2O_3. However, the specimens after scale spallation did not give clear crystal structures after oxidation both in air and O_2. Figures 4(a), (b), (c) and (d) show the XRD spectra of the spalled oxide scales and specimens after scale spallation. The oxidation tests were conducted at 1373K for 180,000s.

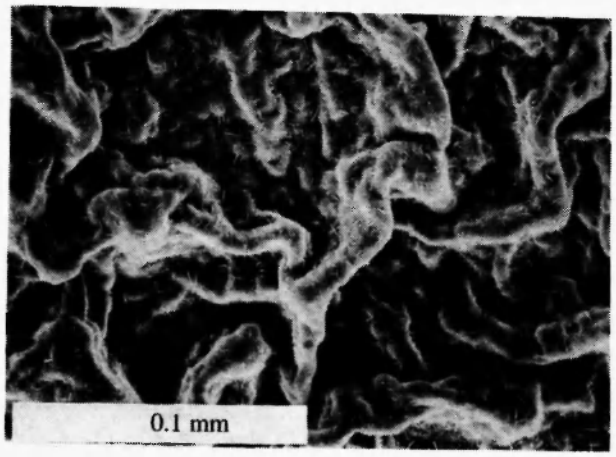

(a)

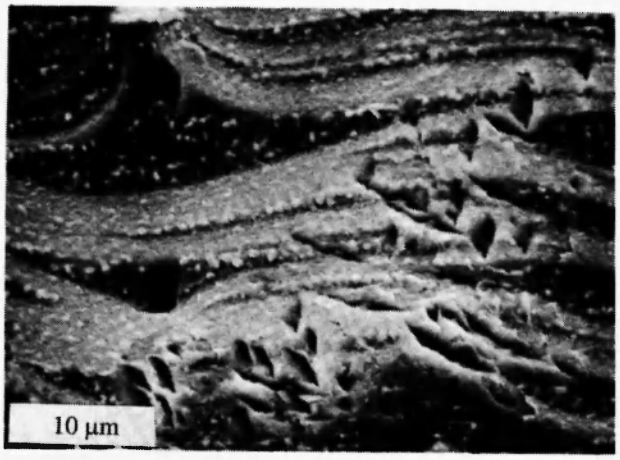

(b)

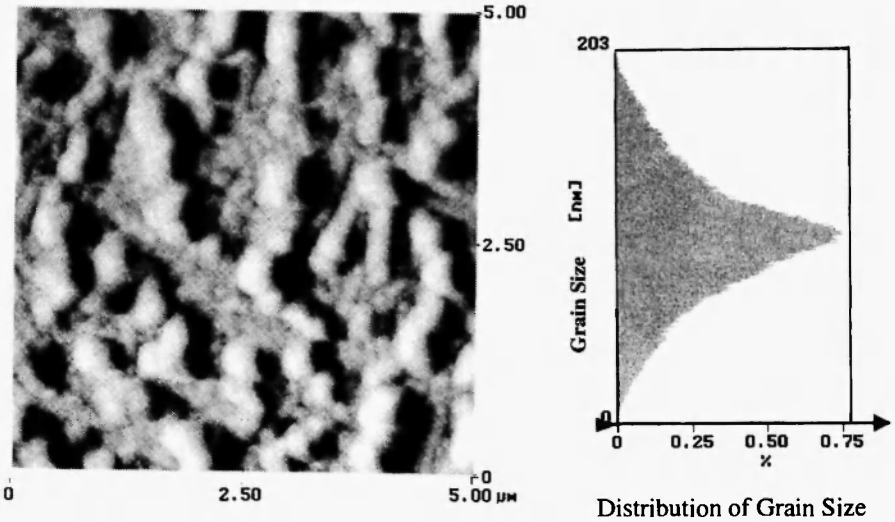

(c)

Fig. 2: Morphology of Fe-37Al oxidised in ambient air at 1373K for 180,000s: (a) a spalled oxide scale, (b) specimen surface after scale spallation, and (c) AFM image showing the grain size of the thin, inner oxide layer

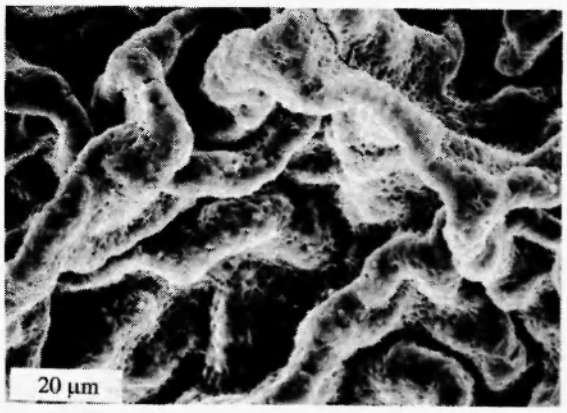

(a)

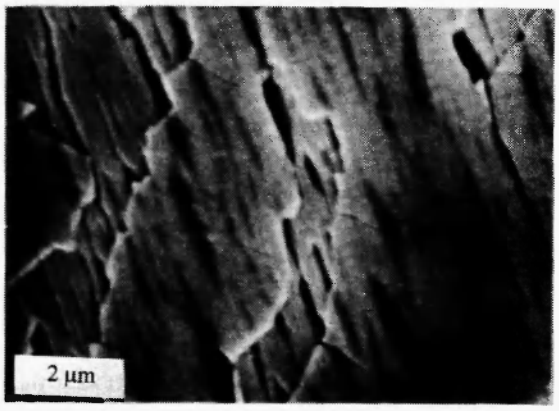

(b)

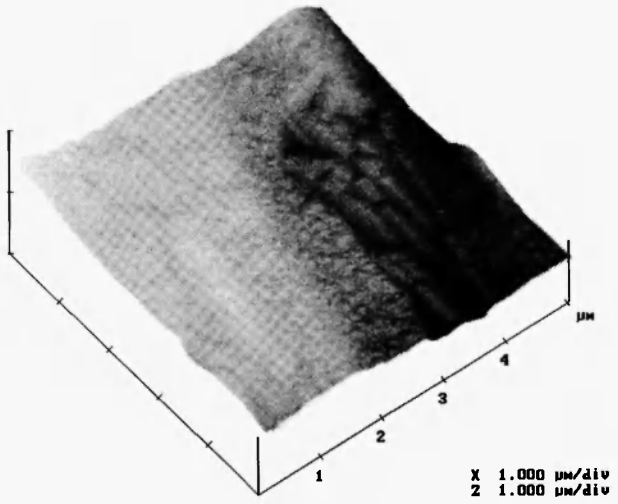

(c)

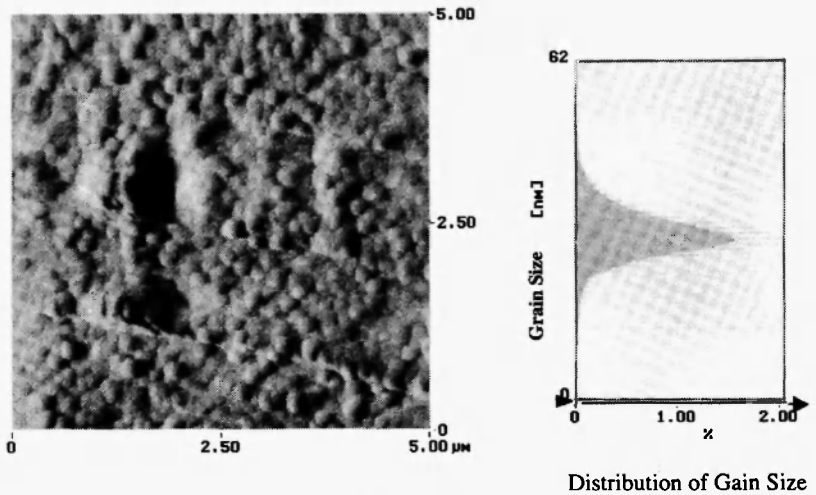

(d)

Fig. 3: Morphologies of Fe-37Al specimens oxidised in oxygen at 1373K for 180,000s: (a) the spalled oxide scale, (b) specimen surface after scale spallation, (c) AFM image of (b), and (d) AFM grain size of the thin, inner oxide layer

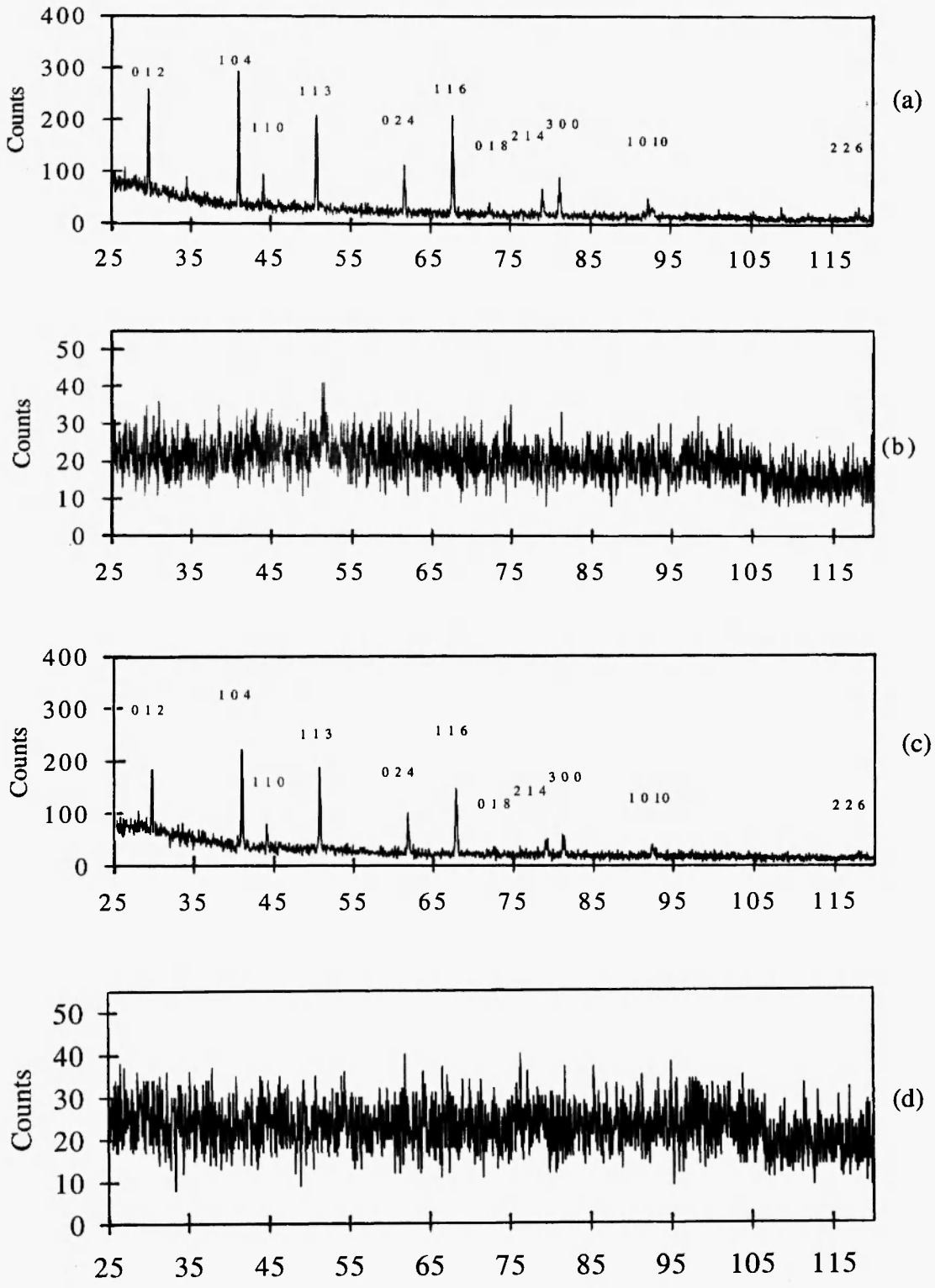

Fig. 4: XRD spectra for the specimens oxidised at 1373K for 180,000s in ambient or oxygen atmospheres. All numbers represent the Miller indices of the planes for α-Al_2O_3. (a) spalled oxide scale from a specimen oxidised in air, (b) the surface of the specimen after scale spallation (oxidised in air), (c) spalled oxide scale from a specimen oxidised in O_2, and (d) the surface of the specimen after scale spallation (oxidised in O_2)

Figure 5 shows the XPS spectra of Fe-37Al oxidised at 1373K for 180,000s after scale spallation. C, Al and O were detected on the surfaces of the specimens oxidised in oxygen, while C, Al, O and N were detected on the specimens oxidised in air. This fact indicated that the reaction products contained N when oxidation took place in ambient air.

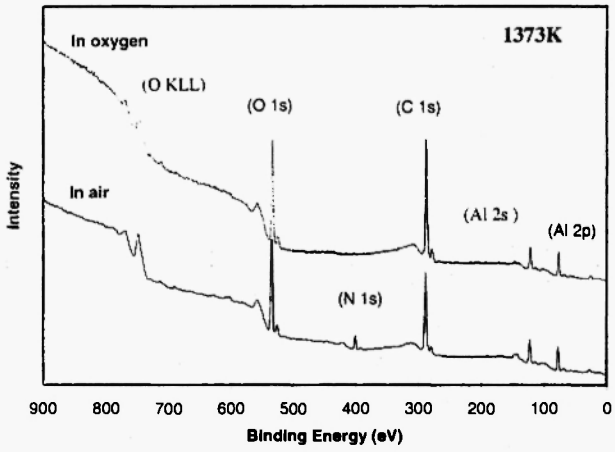

Fig. 5: XPS spectra of Fe-37Al after scale spallation. Oxidation took place at 1373K for 180,000s in ambient air and oxygen.

The absorbed carbon was used as a reference to define the peak shifts. The binding energy of the standard C 1s peak is 285eV. Based on C 1s peak shift, the peak positions for different elements were calculated. Based on the XPS handbook /7/, the Al and O peaks belongs to Al_2O_3. The binding energy of N is close to nitride, suggesting the formation of AlN /8/.

4. DISCUSSIONS

4.1 Oxidation Kinetics

The oxidation kinetics of Fe-37Al at 1273, 1373 and 1473K in air and oxygen were analysed based on the parabolic rate law. The parabolic rate constant (k_p) can be calculated using the weight gain (ΔW), surface area of a specimen (A) and the exposure time (t) by equation (1).

$$(\frac{\Delta W}{A})^2 = k_p t \qquad (1)$$

Figure 6(a), (b) and (c) show the fittings of the parabolic rate law for the isothermal oxidation of FeAl at 1273, 1373 and 1473K, respectively. Although the experimental data deviated from the regression lines, the random scattering was not significant. The parabolic rate constants obtained from the present experiments are listed in Table 1, showing that Fe-37Al has a faster oxidation rate in ambient air than in oxygen. The relative coefficients of the linear regression (R in Table 1) of $(\frac{\Delta W}{A})$ vs t for the oxidation reactions both in air and oxygen were greater than 0.99. The difference between the oxidation rates in oxygen and air is represented by the difference in the values of k_p, which are affected by the oxide structures and doping in the scales.

Using the parabolic rate constant k_p, plots of $log\ k_p$ *vs* $1/T$ for Fe-37Al oxidised in air and oxygen are shown in Figure 7. The activation energy Q can be obtained from the Arrhenius plot (2). The Q value of oxidation in air is lower than that in oxygen, as shown in Table 1.

$$k_p = k_o\ exp(-Q/RT) \qquad (2)$$

where k_p is the parabolic rate constant, R is the gas constant, T is the absolute temperature, and k_o is the pre-exponential factor.

4.2 Oxidation in Ambient and Oxygen Atmospheres

The activation energy of a diffusion process with the vacancy mechanism is the sum of the energy required to form a vacancy and the energy required to move a vacancy from one equilibrium position to another /9/. α-Al_2O_3 is a stoichiometric compound and the defect concentration is very low and difficult to determine. In stoichiometric ionic compounds, the defect equilibrium constant is independent of the O_2 partial pressure /10/. This means that the oxidation rate is dependent on the impurity level in the scales. AlN formed on the inner layer of the oxide scales when Fe-37Al is oxidised in ambient atmosphere /8/. Nitrogen may exist in Al_2O_3 scale as an impurity. According to the defect equilibrium theory, $2N^{-3}$ ions, as an impurity, occupies the $2O^{-2}$ positions in the Al_2O_3. To satisfy electron equilibrium,

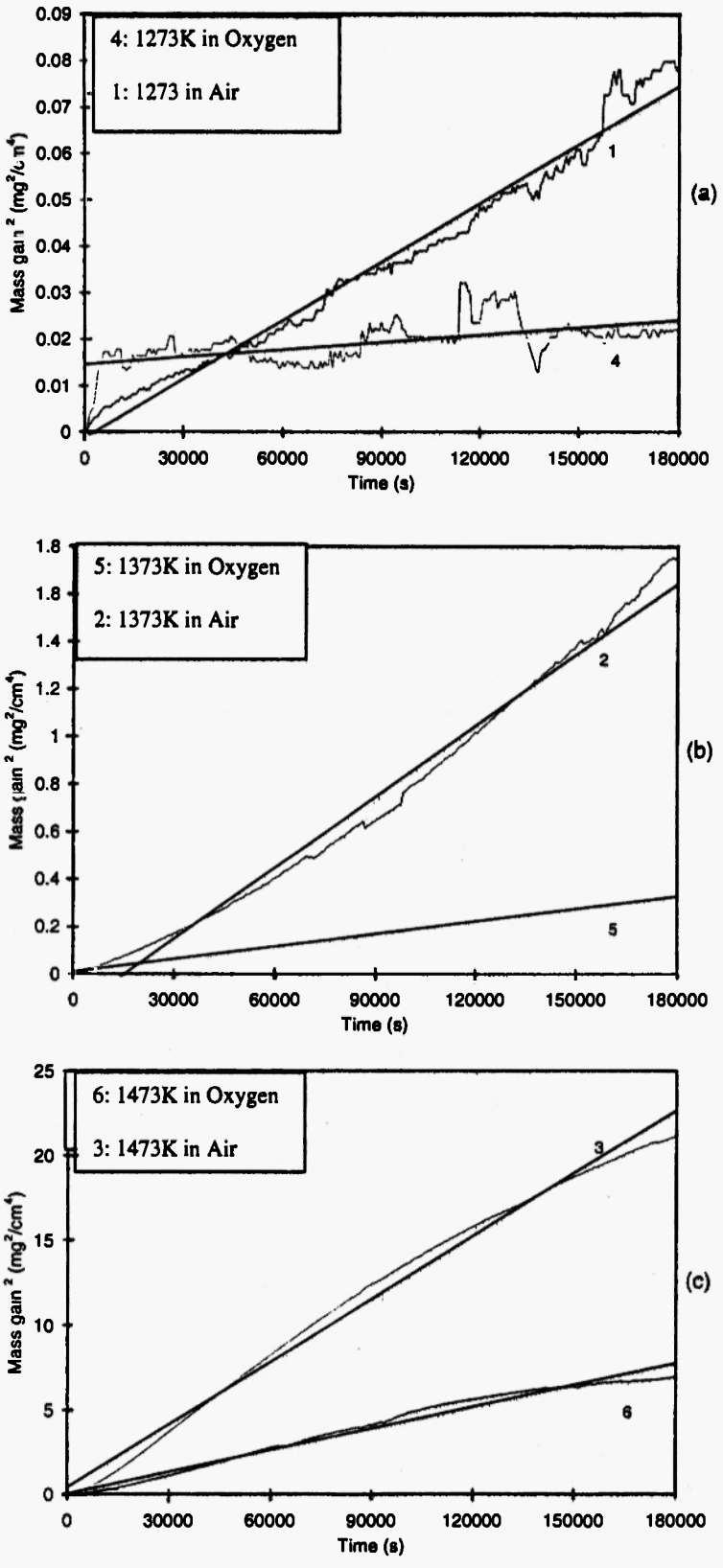

Fig. 6: $\left(\frac{\Delta W}{A}\right)^2$ vs time plots for oxidation of Fe-37Al in air and oxygen at: (a) 1273, (b) 1373 and (c) 1473 K.

Table 1
Parabolic rate constants (k_p) for Fe-37Al specimens oxidised in air and oxygen

Fe-37Al	k_p	$\times 10^{-7}$	$mg^2cm^{-4}s^{-1}$	Q	R
	1273K	1373K	1473K	kJ/mol.	
in air	4.2	99.5	1240	443	0.9995
in oxygen	0.529	17.4	429	522	0.9997

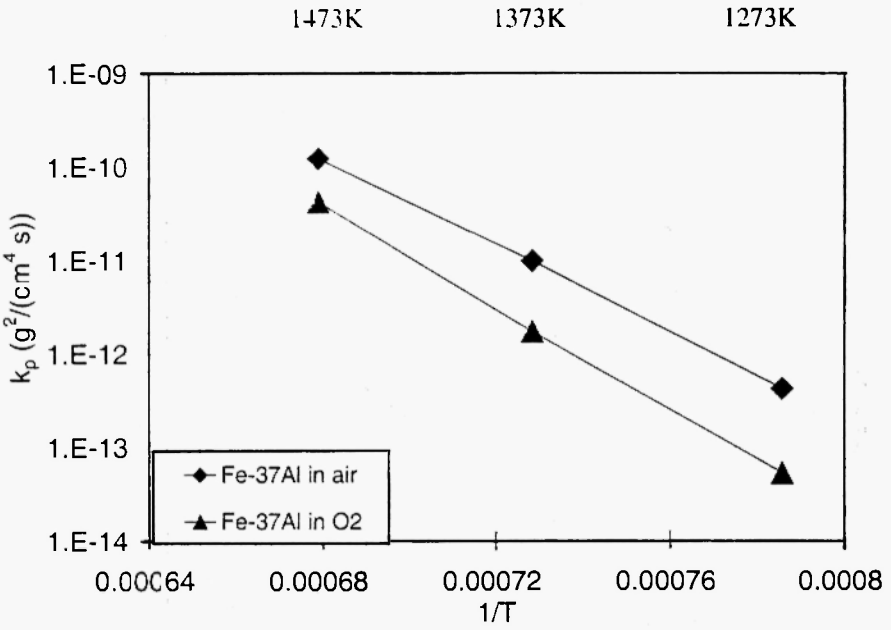

Fig. 7: Arrhenius plots of *log* k_p *vs* $1/T$ for Fe-37Al over the temperature range of 1273 to 1473K in ambient and oxygen atmospheres

one oxygen vacancy is produced to balance the 2 negative electron charges. In this way, nitrogen ions may increase the number of O vacancies, resulting in an increase in the oxygen diffusion rate. Thus the oxidation of FeAl in ambient air shows a faster rate than in oxygen.

Furthermore, it has been shown that some polymorphs of alumina including α-alumina can form in a filamentary shape /11/. The typical filaments are ~20 μm in length and ~0.5 μm in diameter. In the present work, the filamentary oxides formed on Fe-37Al oxidised in ambient air but not in oxygen. It was suggested that a dislocation pipe runs along the axis of each filament /12/. This type of dislocation structure increases the diffusion rates of the species in the oxide, causing an increase of the oxidation rate. This also explains why the oxidation rate of FeAl in air is higher.

5 CONCLUSIONS

The oxidation of Fe-37Al obeys an approximately parabolic rate law at the temperature range of 1273-1473K. The reaction rates were faster in an ambient atmosphere than in pure oxygen. A scale with two-layer structure formed on FeAl specimens during the isothermal oxidation. The outer layer was a convoluted α-Al_2O_3 layer; and the inner layer was a fine-oxide layer with an average grain size of ~30 nm in oxygen and ~100 nm in ambient atmosphere. The

compositions of the inner oxide layers are different for the specimens oxidised in air and oxygen. For oxidation in oxygen, the inner oxide was composed of Al_2O_3; for oxidation in air, the inner oxide consisted of Al_2O_3 + AlN. It is suggested that nitrogen ions in Al_2O_3 increase the diffusion rate of oxygen and therefore the oxidation rate. The filamentary oxides formed on Fe-37Al oxidised in ambient air also have high diffusion rates, increasing the oxidation rate.

ACKNOWLEDGEMENTS

The authors would like to thank the Department of Chemical and Materials Engineering and the Research Centre for Surface and Materials Research for various technical assistance.

REFERENCES

1. J.H. Devan, *Oxidation of High Temperature Intermetallics*, T. Grobstein (ed), Warrendale, PA, TMS, 1989, p.107
2. V.K. Sikka et al., Development and Commercialisation Status of Fe_3Al Based Intermetallic Alloys, *Proc First Int Symp Struct Intermet*, 1993, p.483
3. C.G. McKamey, Development of Iron Aluminides in: *Proceedings of the Fourth Annual Conference on Fossil Energy Materials*, OTNL/FMP-9011, 1990, p.197
4. C-H. Xu and W. Gao, *High Temperature Materials and Processes*, **18** (5-6), 351 (1999)
5. C-H. Xu, Ph.D. Thesis, The University of Auckland, Feb. 1999.
6. C-H. Xu and W. Gao, *Corrosion Science and Protection Technology*, **8** (1), 26, (1996).
7. J.K. Moulder, and J. Chastain, *Handbook of X-ray Photoelectron Spectroscopy*, Eden Prairie, Minn, 1992.
8. C-H. Xu, W. Gao, and Y-D. He, *Scripta Materialia*, **42**, 975-980 (2000).
9. Robert W. Cahn and Peter Haasen, *Physical Metallurgy*, 4th edition, North-Holland, 1996, p.557
10. P. Kofstard, *High Temperature Corrosion*, Elsevier Applied Science, London and New York, 1988, pp.42-54
11. D.J. Barber, *Phil. Mag.*, **10** (103), 75-94 (1964).
12. H.M. Hindham and W.W. Smeltzer, *J. Electrochem. Soc.*, **127** (7), 1630-1635 (1980).